

Behaviors of Flow Index of Dispersed Composite Incompatible Polymer Melts

笠島, 正行 / 伊藤, 勝彦 / IT0, Katsuhiko / KASAJIMA, Masayuki

(出版者 / Publisher)

法政大学工学部

(雑誌名 / Journal or Publication Title)

Bulletin of the Technical College of Hosei University / 法政大学工学部研究集報

(巻 / Volume)

17

(開始ページ / Start Page)

11

(終了ページ / End Page)

21

(発行年 / Year)

1981-03

(URL)

<https://doi.org/10.15002/00004130>

Behaviors of Flow Index of Dispersed Composite Incompatible Polymer Melts

Masayuki KASAJIMA* and Katsuhiko ITO*

Abstract

For dispersed composite incompatible polymer melts, relationships of the flow index to the blended fraction and the temperature shift factor were studied. The various flow indices have large dependency on the shear rate and decrease with increase in the shear rate. None of the combined samples of polypropylene (PP)·high density polyethylene (HDPE) resins, polycarbonate (PC)·poly(methyle methacrylate) (PMMA) resins and of polystyrene (PS)·low density polyethylene (LDPE) resins had a flow index having the additive property. The flow index had unique behavior in that the flow index ($m_{\tau\dot{\gamma}}$) of the blended sample for the PC·PMMA samples became smaller than the $m_{\tau\dot{\gamma}}$ of the monocomponent samples, and which the $m_{\tau\dot{\gamma}}$ of the blended samples for the PS·LDPE samples became larger than the $m_{\tau\dot{\gamma}}$ of the monocomponent samples. However, such unique behavior did not occur in the PP·HDPE samples. For the blended sample, the values of $m_{\tau\dot{\gamma}}$ obtained by the diagrammatical differentiation of the flow characteristic curves and of the temperature shift factor curves agree substantially with each other.

1. Introduction

In the studies^{1)~7)} the relationships between the flow index and property of polymer processing have been investigated. Such relationships include: the relationship between the uniformity^{1), 2)} of T-die extrusions and the flow index; the relationship between the average fluidity³⁾, used in the case where the flow in the mold is investigated, and the flow index. In such studies the flow index is a constant; it is not a function of the shear rate or the shear stress. In other studies^{8)~11)}, It has been reported that the flow index depends on the shear rate. Lately composite polymer materials have been become the center of wide interest. However, the number of studies on the flow characteristics and the flow index of such materials is less than for mono materials. Information on the flow index for composite polymer materials is very useful in the choice, operation, design and development of machines used in the processing of such materials.

In the present work, interrelationships among the flow index, blended fraction, the shear rate and temperature shift factor were investigated.

2. Relationship between Flow Index and Temperature Shift Factor

When measured under a constant shear stress (τ) or at a constant the shear rate ($\dot{\gamma}$), the viscosity (η) has a different value^{10), 13)}. For the dispersed composite incompatible polymer melt, the η is expressed as follows, in the case where the η are functions of

* Department of Mechanical Engineering

the τ , the temperature (T), the hydrostatic pressure (P_h) and the blended fraction (c).

$$\eta = \eta(\tau, T, P_h, c) \quad (1)$$

Assuming that η is a function of $\dot{\gamma}$, T , P_h and c , one obtains,

$$\eta = \eta(\dot{\gamma}, T, P_h, c) \quad (2)$$

The total differentials of Eqs. (1) and (2) are respectively,

$$d\eta = \left(\frac{\partial \eta}{\partial \tau}\right)_{T, P_h, c} d\tau + \left(\frac{\partial \eta}{\partial T}\right)_{\tau, P_h, c} dT + \left(\frac{\partial \eta}{\partial P_h}\right)_{\tau, T, c} dP_h + \left(\frac{\partial \eta}{\partial c}\right)_{\tau, T, P_h} dc \quad (3)$$

$$d\eta = \left(\frac{\partial \eta}{\partial \dot{\gamma}}\right)_{T, P_h, c} d\dot{\gamma} + \left(\frac{\partial \eta}{\partial T}\right)_{\dot{\gamma}, P_h, c} dT + \left(\frac{\partial \eta}{\partial P_h}\right)_{\dot{\gamma}, T, c} dP_h + \left(\frac{\partial \eta}{\partial c}\right)_{\dot{\gamma}, T, P_h} dc \quad (4)$$

where subscript of the parenthesis means a case in which quantity indicated by the subscript is fixed. For a flow under constant hydrostatic pressure, constant shear stress and constant blended fraction, from Eqs. (3) and (4),

$$\left(\frac{\partial \eta}{\partial T}\right)_{\tau, P_h, c} dT = \left(\frac{\partial \eta}{\partial \dot{\gamma}}\right)_{T, P_h, c} d\dot{\gamma} + \left(\frac{\partial \eta}{\partial T}\right)_{\dot{\gamma}, P_h, c} dT \quad (5)$$

The temperature shift factor ($a_{T\tau}$) at a constant shear stress and the temperature shift factor ($a_{T\dot{\gamma}}$) at a constant shear rate are expressed^{(10), (11)} as follows.

$$a_{T\tau}(T, \tau) = \left(\frac{\eta}{\eta_o}\right)_{T\tau} \quad (6)$$

$$= \left(\frac{\dot{\gamma}_o}{\dot{\gamma}}\right)_{T\tau} \quad \because \tau_T = \tau_{T_o} \quad (7)$$

$$a_{T\dot{\gamma}}(T, \dot{\gamma}) = \left(\frac{\eta}{\eta_o}\right)_{T\dot{\gamma}} \quad (8)$$

$$= \left(\frac{\tau}{\tau_o}\right)_{T\dot{\gamma}} \quad \because \dot{\gamma}_T = \dot{\gamma}_{T_o} \quad (9)$$

where subscript o means a value at a reference point. The flow index ($n_{\tau\dot{\gamma}}$) for the τ - $\dot{\gamma}$ flow characteristics is expressed^{(11), (13)} as follows.

$$n_{\tau\dot{\gamma}} = \frac{\partial \ln \tau}{\partial \ln \dot{\gamma}} \quad (10)$$

From Eqs. (5)~(10) and Eq. (11) which express a relationship among the τ , η and $\dot{\gamma}$, one obtains Eq. (12).

$$\tau(\dot{\gamma}) = \eta(\dot{\gamma}) \cdot \dot{\gamma} \quad (11)$$

$$\left(\frac{\partial \ln a_{T\dot{\gamma}}}{\partial \ln a_{T\tau}}\right)_{P_h, c} = (n_{\tau\dot{\gamma}})_{T, P_h, c} \quad (12)$$

The formula of Eq. (12) can be used for the flow characteristics of every kind of fluid. In the case where the method of time-temperature reduced variables is applicable, the $a_{T\tau}$ is equal to the shift factor (a_T). Hence, substituting $a_{T\tau} = a_T$ into Eq. (12), an equation representing the relationship between the flow index and the temperature shift factor can be obtained.

It is known^{(9), (10), (15)} that a relationship between the $n_{\tau\dot{\gamma}}$ and the $\dot{\gamma}$ can be expressed by the formula of Eq. (13).

$$n_{\tau\dot{\gamma}} = \sum_{j=0}^i (\alpha_{\tau\dot{\gamma}})_{o,j} \{\ln(a_T a_P \dot{\gamma})\}^j \quad (13)$$

where α means a constant, a_p means the pressure shift factor, subscript \circ means a value under the reference temperature and the reference pressure. In the case where $n_{\tau\dot{\gamma}}$ is expressed by Eq. (13), the flow index ($m_{\tau\dot{\gamma}}$) introduced from Kasajima et al.'s non-Newtonian fluid model^{9), 10), 15)} is as follows.

$$m_{\tau\dot{\gamma}} = \sum_{j=0}^i \left[\frac{(\alpha_{\tau\dot{\gamma}})_{\circ j}}{j+1} \sum_{k=0}^j \{ \ln(a_T a_p \dot{\gamma}) \}^{j-k} (\ln \dot{\gamma}_{\circ})^k \right] \quad (14)$$

where superscript \circ means a value under standard state. From Eqs. (12)~(14), one obtains,

$$\frac{1}{2} \left\{ \frac{\partial \ln a_{T\dot{\gamma}}}{\partial \ln a_{T\tau}} + (n_{\tau\dot{\gamma}})_{\tau^{\circ}} \right\}_{P_h, c} = (m_{\tau\dot{\gamma}})_{T, P_h, c} \quad (15)$$

In addition, Eq. (15) can be expressed with subscript $\dot{\gamma}^{\circ}$ instead of subscript τ° .

3. Experimental

Various flow indices (m) were obtained by analyzing the data of the flow characteristics reported in previous papers^{12), 16)}. Combinations of incompatible resins are used as follows respectively. Polypropylene resin (PP, NOBLENE S501 of Sumitomo Chemical Industry) and high density polyethylene resin (HDPE, SUMIKATHENE HARD 2705 of Sumitomo Chemical Industry), polycarbonate resin (PC, PANLITE K-1300 of Teijin Chemical) and poly(methyl methacrylate) resin (PMMA, ACRYPET MD of Mitsubishi Rayon), polystyrene resin (PS, STYRON 666 of Asahi Dow) and low density polyethylene resin (LDPE, POLYETHYLENE M 1820 of Asahi Dow).

The blended fraction^{17), 18)} (c) is defined as the weight fraction of the component having low fluidity. In this report, the notation for combined sample will be written so that the resin with the lower fluidity is the first component. The method of obtaining the various indices $m_{\tau\dot{\gamma}}$ and $m_{\eta\dot{\gamma}}$ from each of the τ - $\dot{\gamma}$ flow characteristics is abbreviated here, because such method was reported in the previous papers^{15), 19)}.

4. Results and Discussion

For each of the combined samples relationships between the $m_{\tau\dot{\gamma}}$ and the $\dot{\gamma}_w$ (subscript w means a value at the wall), obtained from the $\ln \tau_w$ - $\ln \dot{\gamma}_w$ flow characteristic curves, as a parameter the c are as follows. The results are shown in Figs. 1~3 for the PP·HDPE, PC·PMMA and PS·LDPE samples respectively. It is seen from Figs. 1~3 that the $m_{\tau\dot{\gamma}}$ decrease with increase in the $\dot{\gamma}_w$ each of the combined samples. The samples of each of the blended fractions relationship between the $m_{\tau\dot{\gamma}}$ and $\ln \dot{\gamma}_w$ can be approximately shown by the straight line in the range measured (the measurement is restricted because melt fracture occurs at higher values of $\dot{\gamma}_w$). The straight lines shown in Figs. 1~3 are cases of Eq. (14) at $i=1$.

For the PP·HDPE samples the $m_{\tau\dot{\gamma}}$ - $\ln \dot{\gamma}_w$ straight lines having different value of c do not intersect with each other and lie, in order of value of c , between the straight lines of PP ($c=1.00$) and HDPE ($c=0$) monocomponent samples. However, slopes of

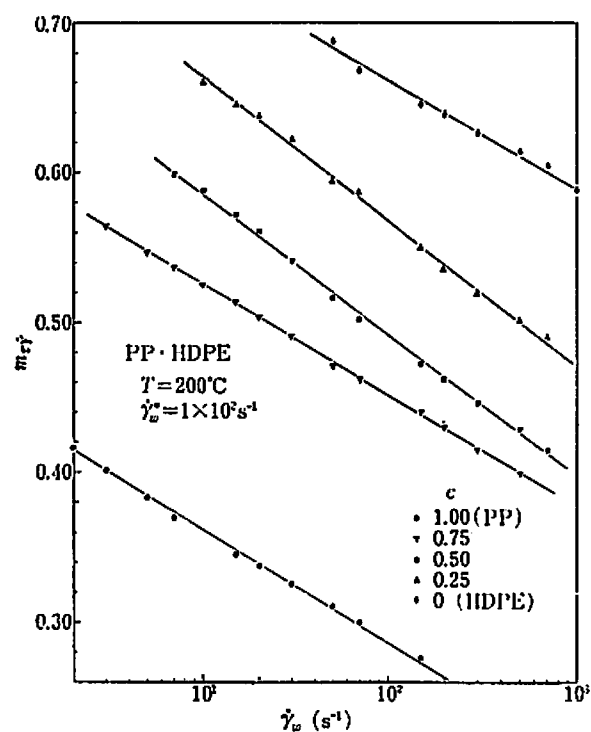


Fig. 1 Relationships between flow index ($m_{\tau\dot{\gamma}}$) and shear rate ($\dot{\gamma}_w$) for PP-HDPE samples at various blended fractions (c).

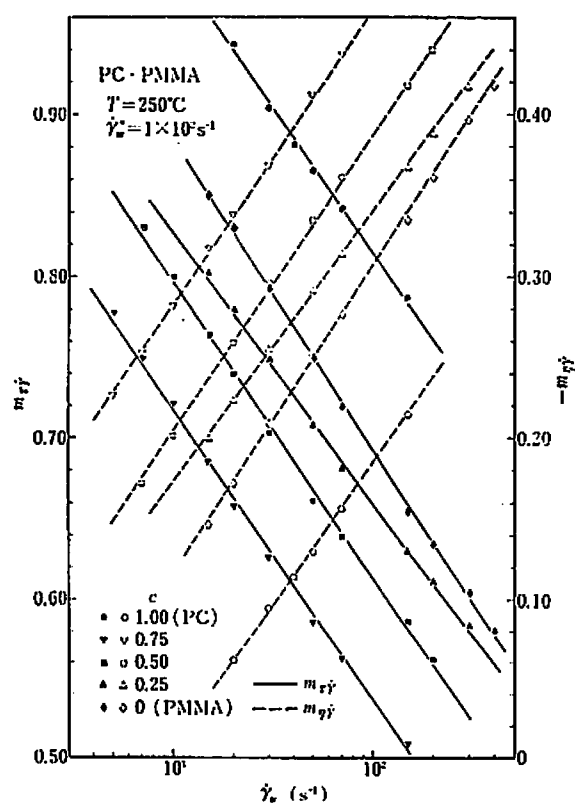


Fig. 2 Relationships flow indices ($m_{\tau\dot{\gamma}}$) and ($m_{\eta\dot{\gamma}}$) relative to shear rate ($\dot{\gamma}_w$) for PC-PMMA samples at various blended fractions (c).

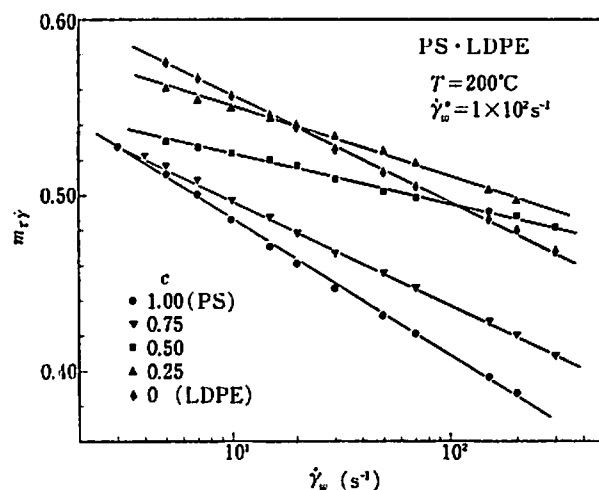


Fig. 3 Relationships between flow index ($m_{\tau\dot{\gamma}}$) and shear rate ($\dot{\gamma}_w$) for PS-LDPE samples at various blended fractions (c).

the $m_{\tau\dot{\gamma}}-\ln \dot{\gamma}_w$ straight lines of each c are not in order of value of the c . The slopes of straight lines of $c=1.00$, 0.75 and 0 are substantially similar to each other. The slopes of straight lines of $c=0.50$ and 0.25 are somewhat larger than $c=1.00$, 0.75 and 0. For the PC-PMMA samples the $m_{\tau\dot{\gamma}}-\ln \dot{\gamma}_w$ relations can also be indicated by the straight lines. The $\dot{\gamma}_w$ dependency of $m_{\tau\dot{\gamma}}$ for the PC-PMMA samples is larger than that for the PP-HDPE samples. When the value of $\dot{\gamma}_w$ changes from one figure for the PC-PMMA sample, the value of $m_{\tau\dot{\gamma}}$ changes approximately 0.2. The slopes of $m_{\tau\dot{\gamma}}-\ln \dot{\gamma}_w$ straight lines, that is, the $\dot{\gamma}_w$ dependency of the $m_{\tau\dot{\gamma}}$ of the various blended fractions are not much different from each other. However, those lines do not be situation in order of the value of c . And the lines of $c=1.00$ (PC monocomponent sample), $c=0$ (PMMA monocomponent sample), $c=0.25$ and 0.75 run from the upward to downward. Namely, some lines of blended samples go beyond the line of monocomponent. The relationships between the $m_{\tau\dot{\gamma}}-\ln \dot{\gamma}_w$ straight lines of the PS-LDPE samples and the blended fraction therefor is not clear. Those lines of the various blended fractions have different slopes, and some lines intersect. In the range of $\dot{\gamma}_w \approx 3 \sim 18 \text{ s}^{-1}$ the $m_{\tau\dot{\gamma}}-\ln \dot{\gamma}_w$ straight lines lie in order of the value c , but in the other range such lines do not. The slope of $m_{\tau\dot{\gamma}}-\ln \dot{\gamma}_w$, that is, the $\dot{\gamma}_w$ dependency of the $m_{\tau\dot{\gamma}}$ is the largest for the PS monocomponent sample ($c=1.00$) and the second largest is for the LDPE monocomponent sample ($c=0$); the slope is on the order of $c=0.75$, 0.25 and 0.50. It is seen that behavior of the $m_{\tau\dot{\gamma}}-\dot{\gamma}_w$ differs with blended fraction.

The profiles of the $m_{\tau\dot{\gamma}}-\ln \dot{\gamma}_w$ lines for PP-HDPE, PC-PMMA and PS-LDPE samples are in contrast to each other. The largest $\dot{\gamma}_w$ dependency of the $m_{\tau\dot{\gamma}}$ is for the PC-PMMA samples. The $m_{\tau\dot{\gamma}}-\ln \dot{\gamma}_w$ lines for the PP-HDPE samples are arranged in order of value of the blended fraction, but for the PC-PMMA and PS-LDPE samples, it is not. Intervals of the $m_{\tau\dot{\gamma}}-\ln \dot{\gamma}_w$ straight lines of the various blended fractions are considerably broad for the PP-HDPE samples, and become narrower for the PC-PMMA and PS-LDPE samples than for the PP-HDPE samples. Hence, influence of the blended fraction on the $m_{\tau\dot{\gamma}}$ is largest for the PP-HDPE samples. In the range measured and the comb-

ined samples used in this study, the $m_{\tau\dot{\gamma}}-\ln \dot{\gamma}_w$ relationships are straight.¹ However, if the kind of combined sample is different, it may be that the such relationships are approximated more suitably by curvilinear (using Eq. (14) at further $i=2$).

For the PC·PMMA samples relationships between the $m_{\eta\dot{\gamma}}$ obtained from the $\ln \eta_w-\ln \dot{\gamma}_w$ flow characteristic curves and the $\dot{\gamma}_w$ are plotted in Fig. 2 by using the marks of \bigcirc , ∇ , \square , \triangle and \diamond . The $m_{\eta\dot{\gamma}}$ has a minus value, and decreases with increase in the $\dot{\gamma}_w$. Relationship between $m_{\eta\dot{\gamma}}$ and $m_{\tau\dot{\gamma}}$ is expressed^{15), 19)} by Eq. (16).

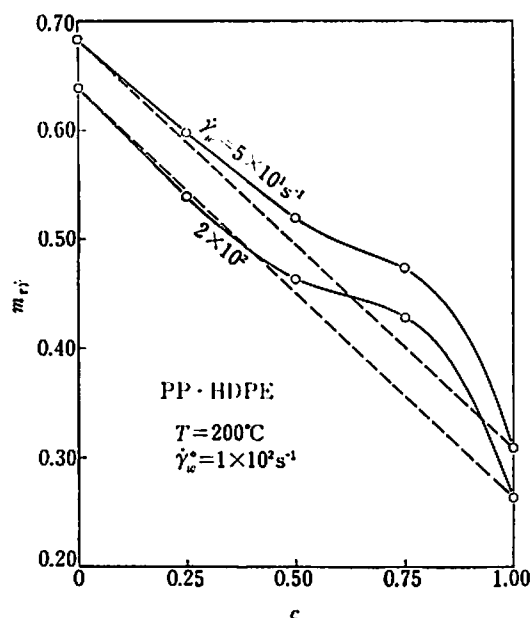


Fig. 4 Flow index ($m_{\tau\dot{\gamma}}$)-blended fraction (c) curves as parameter shear rate ($\dot{\gamma}_w$) for PP·HDPE samples.

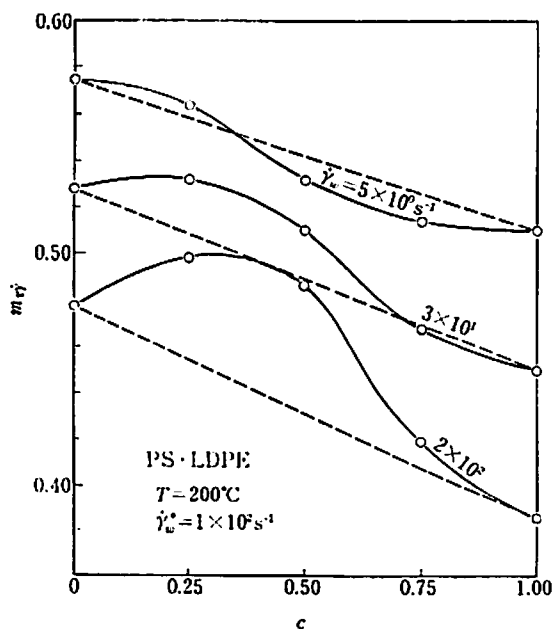


Fig. 6 Flow index ($m_{\tau\dot{\gamma}}$)-blended fraction (c) curves as parameter shear rate ($\dot{\gamma}_w$) for PS·LDPE samples.

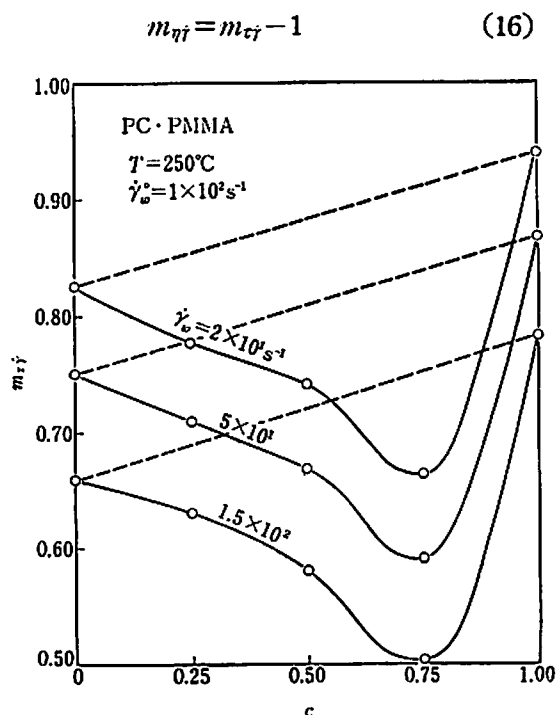


Fig. 5 Flow index ($m_{\tau\dot{\gamma}}$)-blended fraction (c) curves as parameter shear rate ($\dot{\gamma}_w$) for PC·PMMA samples.

The $m_{\eta\dot{\gamma}}$ is obtained from Eq. (16) and the $m_{\tau\dot{\gamma}}-\ln \dot{\gamma}_w$ straight lines shown by the solid lines in Fig. 2. The results are indicated by the broken lines in Fig. 2. It is seen that those broken lines agree substantially with the marks of \bigcirc , ∇ , \square , \triangle and \diamond .

For the various combined samples relationships between the $m_{\tau\dot{\gamma}}$ and the c are shown in Figs. 4~6 using the $\dot{\gamma}_w$ as a parameter. Slopes of the proportional allotment lines indicated by the broken line decrease with in the c . Hence, the c dependency of the $m_{\tau\dot{\gamma}}$ is substantially large. The $m_{\tau\dot{\gamma}}-c$ curves are situated downward along the $m_{\tau\dot{\gamma}}$ ordinate axis with increase in the

$\dot{\gamma}_w$. However, in such case shapes of the curves at the various $\dot{\gamma}_w$ are substantially similar to each other. Slopes of the proportional allotment lines at various $\dot{\gamma}_w$ are also generally similar to each other. At $c=0.25$ and $\dot{\gamma}_w=5 \times 10^1 \text{ s}^{-1}$ the $m_{\tau\dot{\gamma}}-c$ curve keeps off somewhat upward from the proportional allotment line. In the vicinity of $\dot{\gamma}_w=2 \times 10^2 \text{ s}^{-1}$ keeps off somewhat downward from that line. Hence, it is seen that the $m_{\tau\dot{\gamma}}$ of the blended sample is influenced more strongly by the property of PP component than of the HDPE component. At $c=0.50$ the $m_{\tau\dot{\gamma}}-c$ curve separates upwardly from the proportional allotment line. Such phenomenon occurs remarkably in the vicinity of $c=0.75$. These things mean that the $m_{\tau\dot{\gamma}}$ of the blended sample depends strongly on the HDPE component. Additive property of the $m_{\tau\dot{\gamma}}$ does not hold except in the vicinity of $c=0.25$.

For the PC·PMMA samples the $m_{\tau\dot{\gamma}}$ increases with increase in the c . Such thing is the inverse of the behavior of the PP·HDPE samples. When the $\dot{\gamma}_w$ changes, slopes of the proportional allotment lines change very little. With increasing of the $\dot{\gamma}_w$ the lines are situated downward along the $m_{\tau\dot{\gamma}}$ ordinate axis. The $m_{\tau\dot{\gamma}}-c$ curves keep off largely downward from the proportional allotment lines. The minimum value of the $m_{\tau\dot{\gamma}}$ occurs in the vicinity of $c=0.75$. Unique behavior of the flow index, is noted in the value of $m_{\tau\dot{\gamma}}$ of the blended sample, which within the range of $c=0 \sim 0.90$, becomes smaller than that of the PMMA monocomponent sample. The additive property for the PC·PMMA samples does not hold. At $c=0.25$ degree the $m_{\tau\dot{\gamma}}-c$ curve deviation from the proportional allotment line decreases somewhat with increase in the $\dot{\gamma}_w$. At $\dot{\gamma}_w=2 \times 10^1 \text{ s}^{-1}$ the degree of such deviation converted into absolute values of the $m_{\tau\dot{\gamma}}$ is as follows; 0.076 at $c=0.25$, 0.14 at $c=0.50$, 0.246 at $c=0.75$. Thinking that the flow index of the pseudoplastic fluid is usually $0 < m_{\tau\dot{\gamma}} \leq 1$, it is seen that such values are relatively large. That the $m_{\tau\dot{\gamma}}-c$ curves deviate downward from the proportional allotment line rising to the right, means that the $m_{\tau\dot{\gamma}}$ of the blended samples depend strongly on the $m_{\tau\dot{\gamma}}$ of the PMMA sample. Hence, from the property of the monocomponent, it can not simply be analogized that the $m_{\tau\dot{\gamma}}$ value of the blended sample becomes smaller than the $m_{\tau\dot{\gamma}}$ value of the each combined samples. Such unique behavior of the flow index is a new behavior which results from the operation of blending.

For PS·LDPE samples the proportional allotment lines fall to the right and the $m_{\tau\dot{\gamma}}$ decreases with increase in the c . Such behavior is analogous to the case of the PP·HDPE samples. The slopes of the proportional allotment lines increase with increase in the $\dot{\gamma}_w$. Also, those lines are situated like those in which the $m_{\tau\dot{\gamma}}$ decreases with increase in the $\dot{\gamma}_w$. The shapes of the $m_{\tau\dot{\gamma}}-c$ curves for the PS·LDPE samples are changed largely by the $\dot{\gamma}_w$. Under $\dot{\gamma}_w=5 \times 10^0 \text{ s}^{-1}$ the $m_{\tau\dot{\gamma}}-c$ curve at $c=0.25$ is situated upward side from the proportional allotment line, but at $c=0.50$ and 0.75 the curve is situated downward from that line. Hence, in the range of the small c , the $m_{\tau\dot{\gamma}}$ of the blended sample is influenced by the $m_{\tau\dot{\gamma}}$ of the LDPE component. With increase in c it comes to be influenced inversely by the PS component. under $\dot{\gamma}_w=3 \times 10^1 \text{ s}^{-1}$ the $m_{\tau\dot{\gamma}}-c$ curves at $c=0.25$ and 0.50 deviate largely upward from the proportional allotment line and the curve at $c=0.75$ approaches the line. Under $\dot{\gamma}_w=2 \times 10^2 \text{ s}^{-1}$ the $m_{\tau\dot{\gamma}}-c$ curves throughout the

whole range of c are situated upward from the proportional allotment line. As described above, it is seen that the additive property of the flow index does not hold for the PS·LDPE samples. The unique behavior of the flow index in which the $m_{\tau\dot{\gamma}}$ of the blended sample has a larger value than the $m_{\tau\dot{\gamma}}$ of the PS and LDPE monocomponent samples, occurs at $c=0.25$ and 0.50 . Such unique behavior of the flow index is different from the case of the PC·PMMA samples. That is, the unique behavior of the PC·PMMA samples is that the $m_{\tau\dot{\gamma}}$ of the blended sample becomes smaller than the $m_{\tau\dot{\gamma}}$ of each of the mono- components. This unique behavior of the flow index is difficult to estimate from the property of each monocomponent samples.

The patterns of the $m_{\tau\dot{\gamma}}-c$ curves for the PP·HDPE, PC·PMMA and PS·LDPE samples are in fair contrast. For the PP·HDPE and the PS·LDPE samples slopes of the proportional allotment lines drop to the right, that is, the $m_{\tau\dot{\gamma}}$ decreases with increase in the c . For the PC·PMMA samples the slope rises to the right. Looking minutely at the $m_{\tau\dot{\gamma}}-c$ curves for the PP·HDPE samples the $m_{\tau\dot{\gamma}}$ is a decreasing function to c . For the PC·PMMA samples the $m_{\tau\dot{\gamma}}$ at $c=0\sim 0.75$ is a decreasing function to c , but at $c=0.75$ the $m_{\tau\dot{\gamma}}$ is a increasing function. The shapes of the $m_{\tau\dot{\gamma}}-c$ curves for the PP·HDPE and the PC·PMMA samples are not changed much by the $\dot{\gamma}_w$, but for the PS·LDPE samples the curve change is substantial with changing of the $\dot{\gamma}_w$. That is, with in the lower range of $\dot{\gamma}_w$ the $m_{\tau\dot{\gamma}}$ of the blended samples decreases with increase in the c ; with increase in $\dot{\gamma}_w$, the $m_{\tau\dot{\gamma}}$ becomes an increasing function with respect to c and reaches a maximum value; after the $m_{\tau\dot{\gamma}}$ becomes a decreasing function with respect to c . The unique behavior of the flow index occurs without relation to the $\dot{\gamma}_w$ for the PC·PMMA samples, and does not occur within the lower range of $\dot{\gamma}_w$ but does occur within the higher range of $\dot{\gamma}_w$ for the PS·LDPE samples. The unique behavior does not occur

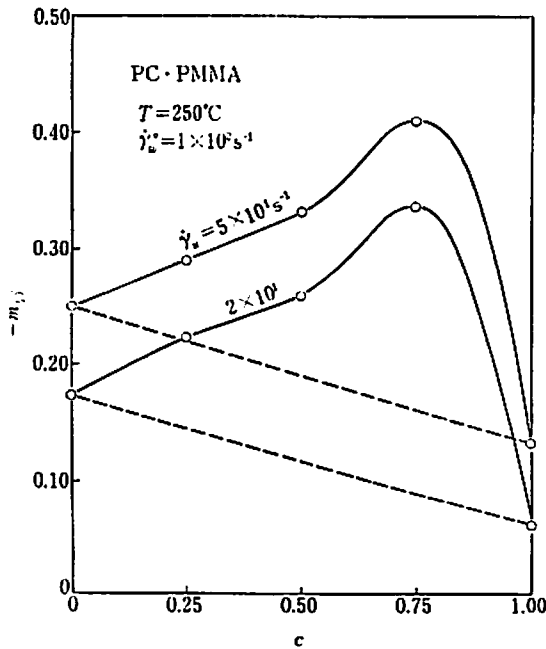


Fig. 7 Flow index ($m_{\tau\dot{\gamma}}$)-blended fraction (c) curves as parameter shear rate ($\dot{\gamma}_w$) for PC·PMMA samples.

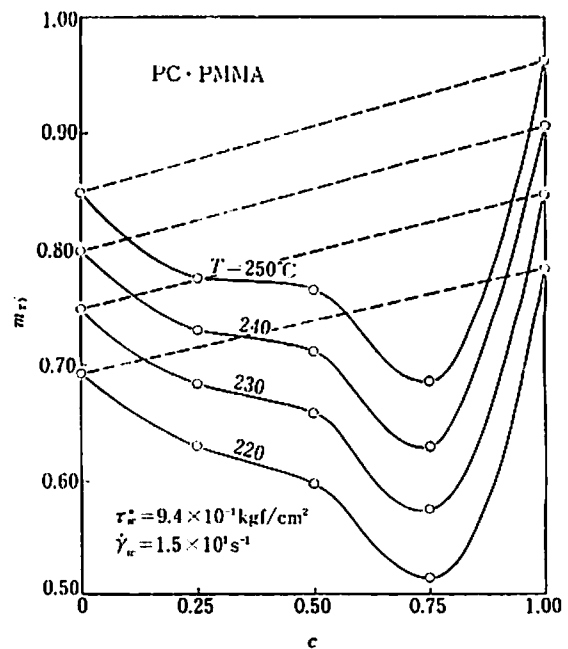


Fig. 8 Flow index ($m_{\tau\dot{\gamma}}$)-blended fraction (c) curves as parameter temperature (T) for PC·PMMA samples.

in the PP·HDPE samples.

Relationships between $m_{\eta\dot{\gamma}}$ and c are shown in Fig. 7. In this figure the $m_{\eta\dot{\gamma}}$ ordinate axis has a minus value. The $m_{\eta\dot{\gamma}}$ decreases with increase in the $\dot{\gamma}_w$. The $m_{\eta\dot{\gamma}}-c$ curves deviate largely from the proportional allotment line. The additive property of the $m_{\eta\dot{\gamma}}$ does not hold in the same manner as the $m_{\tau\dot{\gamma}}$. The unique behavior of the flow index, that is, the $m_{\eta\dot{\gamma}}$ of the blended samples becoming smaller than the $m_{\eta\dot{\gamma}}$ of both PC and PMMA monocomponent samples, occurs for the PC·PMMA samples. The degree to which the $m_{\eta\dot{\gamma}}-c$ curves deviate from the proportional allotment lines increases with increase in c , and becomes maximum in the vicinity of $c=0.75$. However, the shapes of the $m_{\eta\dot{\gamma}}-c$ curves are not changed by the $\dot{\gamma}_w$.

It has been reported^{(10), (19), (20)} that the $m_{\tau\dot{\gamma}}$ depends not only on the $\dot{\gamma}_w$ but also on the temperature (T). For the PC·PMMA samples relationships between the $m_{\tau\dot{\gamma}}$ and the c are shown in Fig. 8 using T as a parameter. The $m_{\tau\dot{\gamma}}-c$ curves at various T deviate largely from the proportional allotment line in the same manner as a case of the $m_{\tau\dot{\gamma}}-c$ curves taking a parameter $\dot{\gamma}_w$, and do not have the additive property. Slopes of the proportional allotment lines increase with increase in T . Amount of the $m_{\tau\dot{\gamma}}-c$ curves deviating from the proportional allotment lines change with changing of the T in the vicinity of $c=0.25$, and are not changed by T at $c=0.75$. Differences in values of $m_{\tau\dot{\gamma}}$ at $T=220^\circ\text{C}$ and 250°C are as follows. Those values are 0.156 at $c=0$, 0.170 at $c=0.75$ and 0.180 at $c=1.00$. Hence, it is seen that the $m_{\tau\dot{\gamma}}$ is influenced strongly by temperature. Within the temperature range measured the $m_{\tau\dot{\gamma}}$ of the blended samples is smaller than the $m_{\tau\dot{\gamma}}$ of both monocomponent samples, and has minimum value in the vicinity of $c=0.75$.

The unique behavior of the flow index can not be presumed simply from the properties of the respective monocomponent samples, and is a new behavior which occurs upon blending incompatible resins. Such unique behavior is a phenomenon of interest in the field of engineering. Phenomena similar to the unique behavior of the flow index have been reported as the unique flow behavior^{(12), (16), (18)} in flow characteristics and the unique kneading behavior^{(21), (22)} in kneading characteristics. However, the mechanism of and correlation of these unique behaviors are not clear as yet.

The monocomponent sample relationships among the $a_{T\dot{\gamma}}$, $a_{T\tau}$ and the $n_{\tau\dot{\gamma}}$ were reported in the previous paper⁽¹¹⁾. However, such relationships for the blended samples have not been reported. Relationships between $a_{T\dot{\gamma}}$ and $a_{T\tau}$ at $c=0.50$ and the reference temperature (T_o)= 220°C for the PC·PMMA samples are shown in Fig. 9 using the shear rate ($\dot{\gamma}_{w0}$) as a parameter. Values of the $a_{T\dot{\gamma}}$ and $a_{T\tau}$ decrease with rise in temperature. The $\ln a_{T\dot{\gamma}}-\ln a_{T\tau}$ curves are upwardly convex, and drop to the right. With increase in the $\dot{\gamma}_{w0}$, the $\ln a_{T\dot{\gamma}}-\ln a_{T\tau}$ curves move upward having a center at the point of $a_{T\dot{\gamma}}=a_{T\tau}=1$. The $m_{\tau\dot{\gamma}}$ are obtained from the $\ln a_{T\dot{\gamma}}-\ln a_{T\tau}$ curves shown in Fig. 9, Eq. (12) and Eq. (15). The results are indicated by the marks of ∇ , \square and \triangle in Fig. 10. Also, the $m_{\tau\dot{\gamma}}$ obtained from the $\tau_w-\dot{\gamma}_w$ flow characteristic curves at various temperatures are indicated by the marks of \bullet , \blacktriangledown , \blacksquare and \blacktriangle in Fig. 10. For the blended samples it is

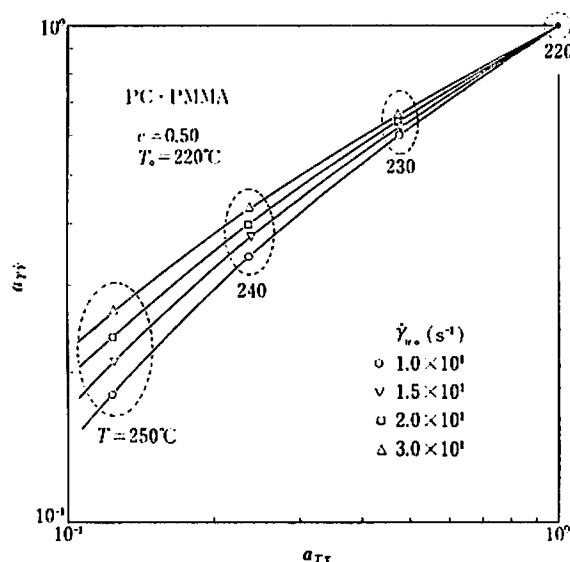


Fig. 9 Relationships between temperature shift factor ($a_{T\dot{\gamma}}$) at constant shear rate and temperature shift factor ($a_{T\tau}$) at constant shear stress for PC-PMMA samples.

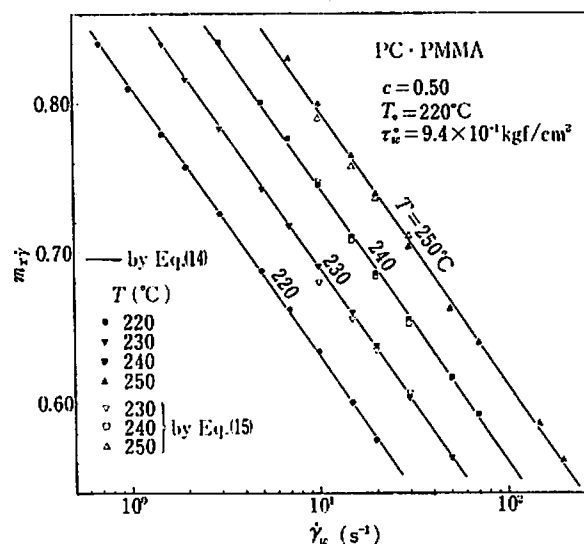


Fig. 10 Relationships between flow index ($m_{T\dot{\gamma}}$) and shear rate ($\dot{\gamma}_w$) for PC-PMMA samples at various temperatures (T).

seen that the $m_{T\dot{\gamma}}$ obtained by various methods of calculation agree substantially with one another. Solid lines shown in Fig. 10 indicate a case in which relationships between the $m_{T\dot{\gamma}}$ and the $\dot{\gamma}_w$ are approximated by a straight line, that is, Eq. (14) at $i=1$. With rise in temperature, the $m_{T\dot{\gamma}}-\dot{\gamma}_w$ line shifts toward increasing of the $\dot{\gamma}_w$.

5. Conclusion

The following points have been brought to light as a result of investigation of flow index of dispersed incompatible polymer melts.

(1) The flow index depends largely on the shear rate. The $m_{T\dot{\gamma}}-\ln \dot{\gamma}_w$ and $m_{T\dot{\gamma}}-\ln \dot{\gamma}_w$ relationships are represented by straight lines. Dependency of the $m_{T\dot{\gamma}}$ on shear rate is larger for the PC-PMMA samples than for the PP-HDPE and PS-LDPE samples. The $m_{T\dot{\gamma}}-\ln \dot{\gamma}_w$ lines are aligned in order of value of the blended fraction for the PP-HDPE samples but not for PC-PMMA and PS-LDPE samples. None of PP-HDPE, PC-PMMA and PS-LDPE have the additive property.

(2) There are two patterns of flow index unique behavior. For the PC-PMMA samples the $m_{T\dot{\gamma}}$ of the blended sample becomes smaller than the $m_{T\dot{\gamma}}$ of each of the monocomponents. For the PS-LDPE samples the $m_{T\dot{\gamma}}$ of the blended sample becomes larger than of each of the monocomponents. For the PC-PMMA samples the occurrence of such unique behavior has no relation to the shear rate, and it occurs remarkably in the vicinity of $c=0.75$. For the PS-LDPE samples such unique behavior do not occur within the lower range of the shear rate, but occurs with increase in the shear rate. For the PP-HDPE samples the unique behavior of the flow index does not occur.

(3) For the blended sample the values of $m_{T\dot{\gamma}}$ obtained by the diagrammatical

differentiation of the flow characteristic curves and of the temperature shift factor curves agree substantially with each other.

References

- 1) J.M. McKelvey and K. Ito, *Polym. Eng. Sci.*, **11**, 258 (1971).
- 2) K. Ito, *Plastic, Japan*, **22**, No. 12, 10 (1971).
- 3) K. Ito, *Kikai no Kenkyu*, **18**, No. 11, 59 (1966).
- 4) H.L. Gunnerson and J.P. Gallagher, *Ind. Eng. Chem.*, **51**, 854 (1959).
- 5) Y. Oyanagi and A. Yamaguchi, 22nd Kobunshi Toronkai Koen Yokoshu (1973, Tokyo), p. III-357.
- 6) Y. Oyanagi, Kobunshi Gakkai Plastic Kako Bunkakai Shiryo (1974, Tokyo), p. 3.
- 7) K. Ito, "Oshidashi Seikei yo Die no Sekkei", Kogyo Chosakai, Tokyo (1970), p. 161.
- 8) O. Amano, *Kobunshi Ronbunshu*, **31**, 595 (1974); *ibid.*, **31**, 601 (1974).
- 9) M. Kasajima, Y. Mori and A. Suganuma, *Kagaku Kogaku Ronbunshu*, **1**, 137 (1975).
- 10) M. Kasajima, A. Suganuma, D. Kunii and K. Ito, "Science and Technology of Polymer Processing", Proc. Int. Conf. Polym. Processing, MIT Press, Cambridge (1979), p. 473.
- 11) M. Kasajima, K. Ito, A. Suganuma and D. Kunii, *Kobunshi Ronbunshu*, **37**, 335 (1980).
- 12) M. Kasajima, A. Suganuma, D. Kunii and K. Ito, *Kobunshi Ronbunshu*, **36**, 481 (1979).
- 13) M. Kasajima, A. Suganuma and D. Kunii, 23rd Rheology Toronkai Koen Yokoshu (Oct., 1975, Hiroshima), p. 57.
- 14) J.D. Ferry, *J. Am. Chem. Soc.*, **72**, 3746 (1950).
- 15) M. Kasajima, *Bull. Coll. Eng., Hosei Univ.*, **14**, 13 (1978).
- 16) M. Kasajima, A. Suganuma, D. Kunii and K. Ito, "Science and Technology of Polymer Processing", Proc. Int. Conf. Polym. Processing, MIT Press, Cambridge (1979), p. 508.
- 17) M. Kasajima and Y. Mori, *Kagaku Kogaku*, **37**, 915 (1973).
- 18) M. Kasajima, A. Suganuma, D. Kunii and K. Ito, *J. Soc. Rheology, Japan*, **7**, 27 (1979).
- 19) M. Kasajima and K. Ito, *Bull. Coll. Eng., Hosei Univ.*, **16**, 85 (1980).
- 20) M. Kasajima, *Bull. Coll. Eng., Hosei Univ.*, **14**, 25 (1978).
- 21) M. Kasajima, K. Ito, A. Suganuma and D. Kunii, *Kobunshi Ronbunshu*, **37**, 41 (1980).
- 22) M. Kasajima, K. Ito, A. Suganuma and D. Kunii, *Kobunshi Ronbunshu*, **37**, 419 (1980).